FIGURE LEGENDS

Table 1. Primers for Nmnat3$^{gt/gt}$ mice genotyping and mouse Nmnat3 qPCR. Locations of the primers used in geneotyping for Nmnat3$^{gt/gt}$ mice are indicated in Figure 2A. Locations of the primers used for qPCR of Nmnat3 mRNA are indicated in Figure 2B.

Table 2. Hematological examination reveals Nmnat3$^{gt/gt}$ mice are anemic, but not pancytopenia. Peripheral blood cell numbers and various hematological parameters were counted in 12 weeks old WT and Nmnat3$^{gt/gt}$ mice (n = 4 for each group). All data are expressed as mean ± SD. The abbreviations used are as follows: RBC, red blood cell; Hb, hemoglobin; HCT, hematocrit; MCV, mean corpuscle volume; MCH, mean corpuscle hemoglobin; MCHC, mean corpuscle hemoglobin concentration; WBC, white blood cell; Neu, neutrophil; Lym, lymphocyte; Ba, basophil; Eo, eosinophil; Mo, monocyte; PLT, platelet.

Figure 1. Nmnat3 exists in cytoplasmic fraction of mature erythrocytes. (A) Immunoblot analysis of Nmnat3 expression in indicated tissues from wild-type (WT) mouse. β-Actin, β-Tubulin and GAPDH were used as loading controls. (B) Immunofluorescent images of human NMNAT3-Flag over-expressed Hela cells (Right panel). DsRed2-Mito was co-transfected and used as mitochondrial marker (red). NMNAT3-Flag (green) was visualized by anti-Flag M2 antibody. NMNAT3-Flag expression was also confirmed by Western blotting with anti-Flag M2 antibody (Left panel). (C) Fractionation experiment of mature erythrocyte using WT mouse. GAPDH was used as a cytoplasm fraction marker. Ter119 and β-Actin were used as membrane fraction markers. Nmnat3 was detected in the cytoplasm fraction. (D) Fractionation experiment of reticulocyte using WT mouse. GAPDH was used as a cytoplasm fraction marker. Tom20 was used as mitochondrial fraction markers. Nmnat3 was detected in the cytoplasm fraction.

Figure 2. Nmnat3$^{gt/gt}$ mice exhibit splenomegaly and hemolytic anemia. (A) Map of Nmnat3 gene-trapped allele. The gene-trap cassette was inserted into the indicated point between *Nmnat3* gene exon 1 and exon 2. (B) Structure of Nmnat3 mRNA generated from WT and Nmnat3 gene-trapped allele. The abbreviations used are as follows: SA, splicing acceptor; β-geo, β-galactosidase and neomycin resistance cassette fusion gene; pA, poly-A. (C) Genotyping PCR of Nmnat3 gene-trap homozygous mice (Nmnat3$^{gt/gt}$ mice). Primer sets are shown as green arrow in (A). These primer sets successfully amplified 340 bp, 675 bp and 184 bp PCR products for wild type allele, 5' end and 3' end of gene-targeted allele, respectively. (D-F) Real-time quantitative PCR analysis of Nmnat3 mRNA using primer sets to detect exon1, exon2-3 junction, or exon5. Total RNA was prepared from skeletal muscle (D), heart (E) and liver (F). Data are presented as mean ± SD (n = 4 for each group). (G and H) Immunoblot analysis of Nmnat3 in RBC (G) and skeletal muscle (H) prepared from WT and Nmnat3$^{gt/gt}$ mice. β-Actin or β-Tubulin was used as a loading control. Arrowhead indicates the Nmnat3 band (~30 kDa). (I) Representative picture of spleens from 8-week-old WT and Nmnat3$^{gt/gt}$ mice. (J) Ratio of spleen and body weight was calculated using WT and Nmnat3$^{gt/gt}$ mice (n = 4 for each group). (K) Hematoxylin-Eosin (HE) staining of spleen section prepared from WT and Nmnat3$^{gt/gt}$ mice. Hemosiderin deposit was seen in the enlarged lower left corner. Scale bar represents 50 μm. (L) May-Giemsa and New Methylene Blue staining of peripheral blood collected from WT and Nmnat3$^{gt/gt}$ mice. Scale bar represents 20 μm. (M) Representative scanning electron microscope image of erythrocytes prepared from WT and Nmnat3$^{gt/gt}$ mice. Experiments were independently repeated three times. (N) RBCs of 12-week old mice (n = 3 for each group) were biotinylated by tail vein injection of EZ-Link Sulfo-NHS-biotin and blood was drawn at indicated time. RBC was labeled with phycoerythrin (PE)-conjugated streptavidin and quantified by flow cytometry. Data are presented as mean ± SD. (n = 3 for each group)

Figure 3. Erythropoiesis is compensatory up regulated, but normal in Nmnat3$^{gt/gt}$ mice. (A-C) Flow cytometer analysis for erythroid differentiation stage. Splenocytes (A), bone marrow cells (B), and peripheral blood (C) prepared from 8-week-old WT and Nmnat3$^{gt/gt}$ mice were analyzed by the expression of erythroid cell surface marker Ter119 and CD71 with flow cytometer. The representative data are shown in left panel for each cell types. P4 (Ter119^{high}/ CD71^{high}), P5 (Ter119^{high}/ CD71^{middle}), and P6 (Ter119^{high}/ CD71^{low}) populations were calculated as percent of total (right graph). Data are presented as mean ± SD. (n = 4 for each group) (D) Whole blood cells were stained with Hoechst 33342 and MitoTracker Orange for nucleus and mitochondria, respectively. Cells stained with Hoechst 33342 are indicated by arrow. Phase contrast image (DIC) was shown in left panel.

Figure 4. Nmnat3 is a dominant Nmnat isozyme in mature erythrocytes. (A) Nmnat3-specific activity and total Nmnat activity of mature erythrocytes were determined by discrimination assay with $CoCl_2$ and $MgCl_2$, respectively. For this assay, mature erythrocytes lysates were prepared from WT and Nmnat3$^{gt/gt}$ mice. Samples were dialyzed to remove endogenous metal ion and metabolites. Data are presented as mean ± SD (n = 3 for each group). (B) Immunoblot analysis of endogenous Nmnat1 and Nmnat2 protein in mature erythrocyte with Nmnat1 and Nmnat2 specific antibody. Total cell lysates from mouse Nmnat1 or Nmnat2 over-expressed NIH3T3 cells were used as positive control.

Figure 5. NAD pool in mature erythrocytes is drastically reduced in Nmnat3$^{gt/gt}$ mice. (A) Representative chromatograms of NAD in RBC samples prepared from WT and Nmnat3$^{gt/gt}$ mice. (B and C) Absolute quantification of NAD (B) and NADH (C) level in RBC prepared from 8-week-old WT and Nmnat3$^{gt/gt}$ mice. The concentration was calculated from peak area using standard curve and expressed as defined unit. Data are presented as mean ± SD (n = 4 for each group). (D) Absolute quantification of NAD level in whole blood prepared from 8-week-old WT and Nmnat3$^{gt/gt}$ mice. The concentration was calculated from peak area using standard curve and expressed as defined unit. Data are presented as mean ± SD (n = 4 for each group). (E and F) Semi-quantification of NAD related metabolites in RBC (E) or whole blood (F). NAM (Nicotinamide), NMN (Nicotinamide mononucleotide), NAD (Nicotinamide adenine dinucleotide), NA (Nicotinic acid), NAMN (Nicotinic acid mononucleotide), NAAD (Nicotinic acid adenine dinucleotide), and NR (Nicotinamide riboside) were measured by LC-MS/MS. Data are presented as mean ± SD (n = 4 for each group). N.D. means not detected. (G) NAD amount was measured in heart, liver and skeletal muscle. NAD amount was normalized by wet tissue weight. Data are presented as mean ± SD (n = 4 for each group). (H) Representative result of FACS sorting. Splenocytes from WT and Nmnat3$^{gt/gt}$ mice were stained with anti-CD71-FITC and anti-Ter119-PE, and were sorted by FACS Aria with defined gates. (I) P4 (Ter119^{high}/ CD71^{high}), P5 (Ter119^{high}/ CD71^{middle}), and P6 (Ter119^{high}/ CD71^{low}) sub-populations of splenocytes were sorted, and NAD level in these samples were measured by LC-MS/MS. Data are presented as mean ± SD (n = 4 for each group). (J) Absolute quantification of NADP in RBC. NADP was measured by LC-MS/MS. The concentration was calculated from peak area using standard curve and expressed as defined unit. Data are presented as mean ± SD (n = 4 for each group). (K) Immunoblot analysis of NADK and Nampt in mature erythrocytes from WT and Nmnat3$^{gt/gt}$ mice. β-Actin was used as a loading control. Arrowhead indicates the NADK band (~50 kDa). Proteins were extracted from three mice for each groups. (L) GSH (reduced glutathione) and GSSG (oxidized glutathione) in RBC were measured by LC-MS/MS. Data are presented as mean ± SD (n = 4 for each group).

Figure 6. Glycolysis pathway is blocked in Nmnat3$^{gt/gt}$ erythrocytes. (A) Metabolites in glycolysis pathway and pentose phosphate pathway were measured using RBC samples obtained from 8-week-old WT and Nmnat3$^{gt/gt}$ mice (n = 4 for each group). G6P/F6P (Glucose 6-phospate / Fructose 6-phospate), F1,6BP (Fructose 1,6-bisphosphate), DHAP (Dihydroxyacetone phosphate), GAP (Glyceraldehyde 3-phosphate), 2,3-BPG (2,3-bisphospho glycerate), 3PG (3-phosphoglycerate), PEP

(Phosphoenolpyruvate), PYR (Pyruvate), LAC (Lactate), 6PG (6-phosphogluconate), PRPP (Phosphoribosyl pyrophosphate), R5P/Ru5P (Ribose 5-phosphate / Ribulose 5-phosphate), Xu5P (Xylulose 5-phosphate) and S7P (Sedoheptulose 7-phosphate) were analyzed by MRM based LC-MS/MS method. Data are presented as mean ± SD. (B) Enzymatic activities of glycolysis enzymes were assayed with RBC lysate prepared from 8-week-old WT and Nmnat3$^{gt/gt}$ mice (n = 4 for each group). PFK (phosphofructokinase), ALD (aldolase), PK (pyruvate kinase), HK (hexokinase), GPI (glucose 6-phosphate isomerase), TPI (triose phosphate isomerase), PGK (phosphoglycerate kinase), ENOL (enolase) and LDH (lactate dehydrogenase) were measured by the methods recommended by International Committee for Standardization in Hematology. (C) Immunoblot analysis of PFK and GAPDH in mature erythrocytes from WT and Nmnat3$^{gt/gt}$ mice. β-Actin was used as loading control. Proteins were extracted from three mice for each group. (D) Enzymatic activities of pentose phosphate pathway enzymes (G6PD; glucose 6-phosphate dehydrogenase, 6PGD; 6-phosphogluconolacton dehydrogenase) were assayed with RBC lysate prepared from 8-week-old WT and Nmnat3$^{gt/gt}$ mice (n = 4 for each group). (E) Enzymatic activities of AK (adenylate kinase) and ADA (adenosine deaminase) were assayed with RBC lysate prepared from 8-week-old WT and Nmnat3$^{gt/gt}$ mice (n = 4 for each group). (F) Measurement of Acetyl-CoA level in RBC prepared from WT and Nmnat3$^{gt/gt}$ mice (n = 4 for each group). (G) Acetylation status of erythrocytes protein. RBC lysates were separated by SDS-PAGE and subjected to immuno blotting with acetyl-lysine specific antibodies (Abcam and Cell Signaling). Proteins were extracted from three different mice for each group.

Figure 7. Glucose flow is shifted to pentose phosphate pathway and reversed from GAP to F1,6BP in Nmnat3$^{gt/gt}$ erythrocytes. (A) Primary cultured erythrocytes prepared from WT and Nmnat3$^{gt/gt}$ mice were cultivated in the medium containing [U-13C]-glucose. 13C-labeled metabolites were monitored by MRM based LC-MS/MS method. Samples were harvested at the time point of 0, 30, 60, 90 and 120 min. Data are presented as mean ± SD (n = 4 for each group). (B) Schema of carbon flow by [1,2-13C] glucose tracer analysis. White and red circles are 12C and 13C, respectively. (C and D) Primary cultured erythrocytes prepared from WT and Nmnat3$^{gt/gt}$ mice were cultivated in the medium containing [1,2-13C]-glucose. Different isotopomers of 13C-labeled F1,6BP (C) and R5P/Ru5P (D) were monitored by MRM based LC-MS/MS method. Samples were harvested at the time point of 0, 30, 60, 90 and 120 min. Data are presented as mean ± SD (n = 4 for each group). (E) Measurement of ATP level in whole blood collected from WT and Nmnat3$^{gt/gt}$ mice (n = 4 for each group). Data are presented as mean ± SD.

Figure 8. Schematic of the hemolytic anemia in Nmnat3$^{gt/gt}$ mice. Nmnat3 is the dominant Nmnat among the three isoforms in mature erythrocytes, and its deficiency leads to a drastic depletion of the NAD pool. A lowered NAD level inhibits glycolysis at GAPDH and reverse the glycolytic flow between F1,6BP and GAP. Impaired ATP synthesis in Nmnat3$^{gt/gt}$ erythrocytes leads to the dysfunction of Na^+-K^+-ATPase and a resulting spiked shaped erythrocytes, which are preferentially trapped and destroyed by the reticuloendothelial system of the spleen. Thus, Nmnat3 deficiency in mice caused splenomegaly and hemolytic anemia.

Table 1

Genotyping primers for Nmnat3$^{gt/gt}$ mice	
Primer #1	TCTTCTGGGGTCGCAGTTAT
Primer #2	CCTTCTTTCTGGTCTTTCTCTGTGCAA
Primer #3	TGCCACCTGACGTCTAAGAA
Primer #4	GACAGTGCAGCGATGTCCTA
qPCR primers for mouse Nmnat3	
Nmnat3-Ex1	FWD: GTGTCCACGAAGCCTTGAGT
	REV: CAGCCATCTGACTCTGTCGT
Nmnat3-Ex2-3	FWD: CACCAAACAGGAAGGTACCA
	REV: AAGCCACCAGGTCTTTCTTC
Nmnat3-Ex5	FWD: CAGGGTTCCCAATATCCTGA
	REV: TCAAACAAGCAGGCAGTCAT
B2m (Beta-2-microglobulin)	FWD: TTCTGGTGCCTTGTCTCACTGA
	REV: CAGTATGTTCGGCTTCCCATTC
Rpl13a (ribosomal protein L13a)	FWD: AGCGCCTCAAGGTGTTGGA
	REV: GAGTGGCTGTCACTGCCTGGTA

Table 2

Peripheral blood cell count

	WT	Nmnat3$^{gt/gt}$	*p* value
RBC (×10^4/μL)	730±12.2	483±11.8	p<0.0001
Hb (g/dL)	11.2±0.299	7.70±0.141	p<0.0001
Ht (%)	37.0±0.825	25.4±0.480	p<0.0001
MCV (fL)	50.7±0.804	52.6±0.545	p<0.05
MCH (pg)	15.4±0.258	16.0±0.206	p<0.05
MCHC (%)	30.4±0.311	30.4±0.386	n.s.
WBC (×10^2/μL)	24.3±5.44	16.8±5.68	n.s.
Neu (%)	17.3±3.40	13.0±3.56	n.s.
Lym (%)	78.0±5.29	84.5±3.79	n.s.
Ba (%)	0.00±0.00	0.00±0.00	n.s.
Eo (%)	2.00±1.83	1.00±0.82	n.s.
Mo (%)	2.75±0.96	1.50±1.29	n.s.
PLT (×10^4/μL)	87.3±7.83	76.2±2.62	n.s.
Reticulocyte (‰)	36.0±1.41	236±10.2	p<0.0001

Figure 1

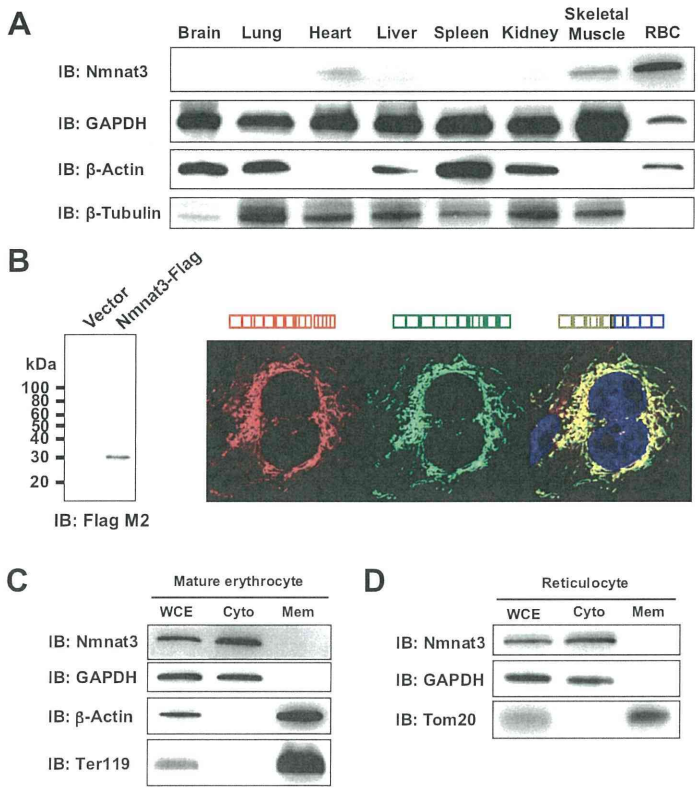

Figure 2

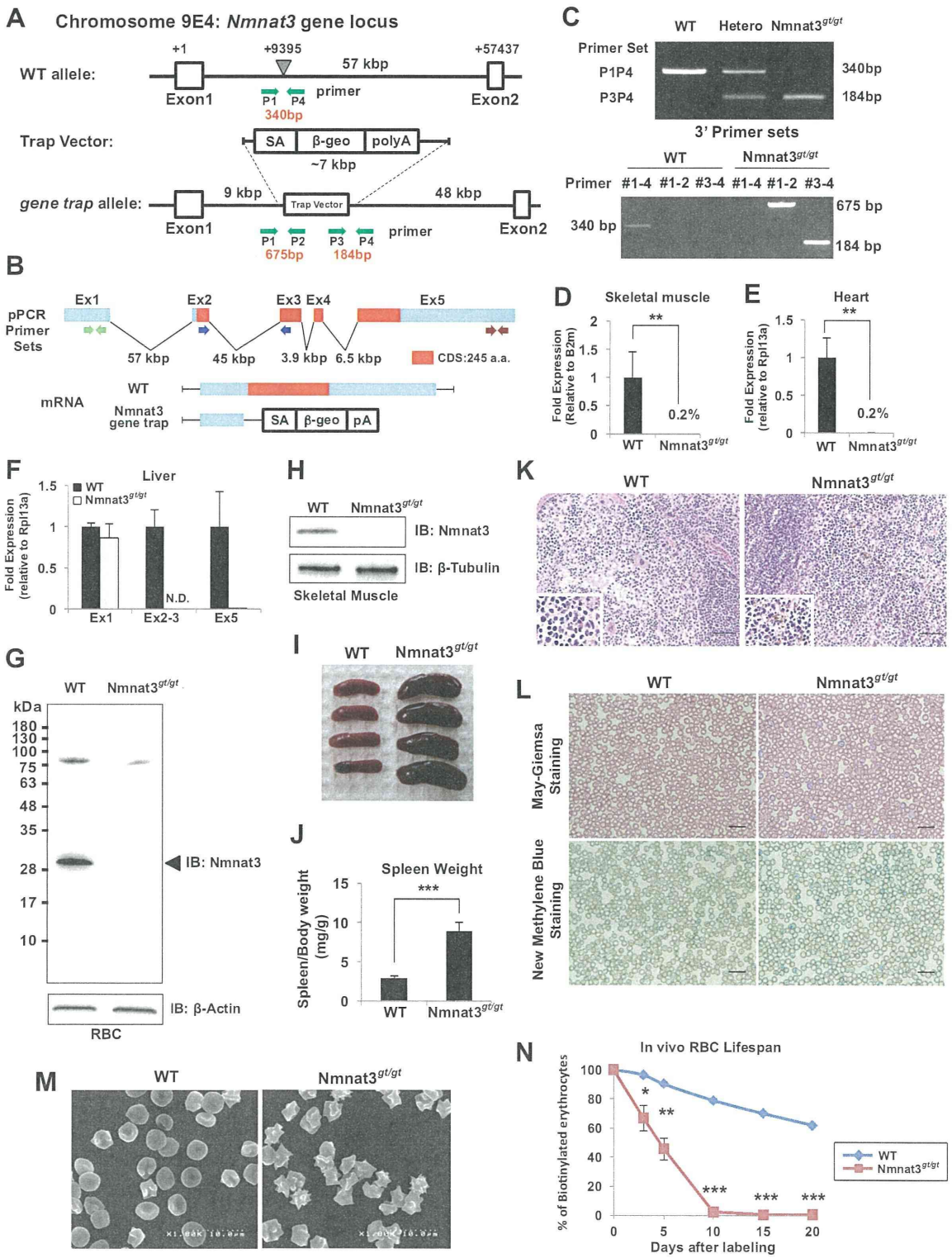

Figure 3

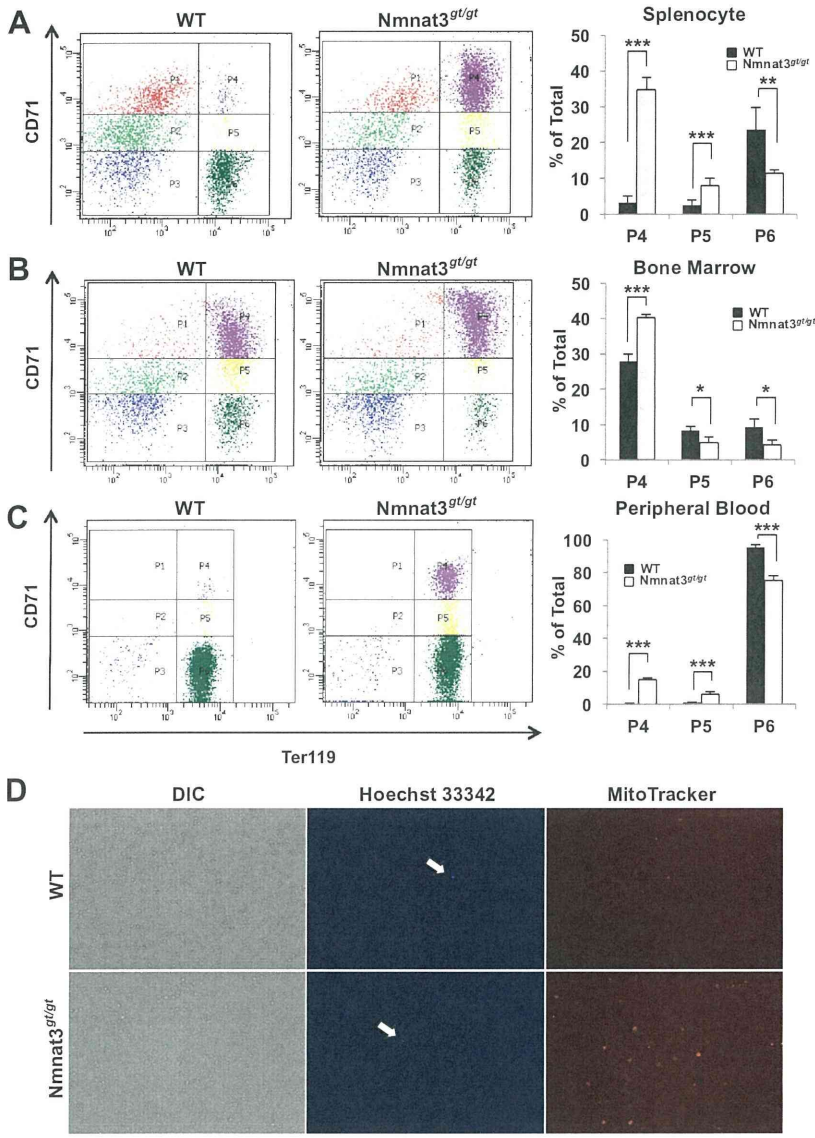

Figure 4

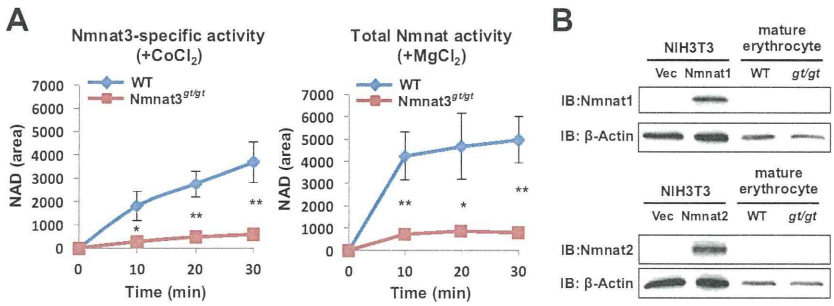

Figure 5